#### **ORIGINAL PAPER**



# Experimental investigation into L-Arg and L-Cys eco-friendly surfactants in enhanced oil recovery by considering IFT reduction and wettability alteration

Hamed Foroughi Asl<sup>1</sup> · Ghasem Zargar<sup>1,2</sup> · Abbas Khaksar Manshad<sup>1</sup> · Mohammad Ali Takassi<sup>2</sup> · Jagar A. Ali<sup>3,4</sup> · Alireza Keshayarz<sup>5</sup>

Received: 12 April 2019 © The Author(s) 2019

#### **Abstract**

Surfactant flooding is an important technique used to improve oil recovery from mature oil reservoirs due to minimizing the interfacial tension (IFT) between oil and water and/or altering the rock wettability toward water-wet using various surfactant agents including cationic, anionic, non-ionic, and amphoteric varieties. In this study, two amino-acid based surfactants, named lauroyl arginine (L-Arg) and lauroyl cysteine (L-Cys), were synthesized and used to reduce the IFT of oil-water systems and alter the wettability of carbonate rocks, thus improving oil recovery from oil-wet carbonate reservoirs. The synthesized surfactants were characterized using Fourier transform infrared spectroscopy and nuclear magnetic resonance analyses, and the critical micelle concentration (CMC) of surfactant solutions was determined using conductivity, pH, and turbidity techniques. Experimental results showed that the CMCs of L-Arg and L-Cys solutions were 2000 and 4500 ppm, respectively. It was found that using L-Arg and L-Cys solutions at their CMCs, the IFT and contact angle were reduced from 34.5 to 18.0 and 15.4 mN/m, and from 144° to 78° and 75°, respectively. Thus, the L-Arg and L-Cys solutions enabled approximately 11.9% and 8.9% additional recovery of OOIP (original oil in place). It was identified that both amino-acid surfactants can be used to improve oil recovery due to their desirable effects on the EOR mechanisms at their CMC ranges.

 $\textbf{Keywords} \ \ Chemical \ EOR \cdot Amino-acid \ surfactant \cdot IFT \cdot Wettability \cdot Coreflooding$ 

## Edited by Yan-Hua Sun

☐ Ghasem Zargar gzha.nano113@gmail.com

Published online: 26 July 2019

- Department of Petroleum Engineering, Abadan Faculty of Petroleum Engineering, Petroleum University of Technology (PUT), Abadan, Iran
- Department of Petroleum Engineering, Ahwaz Faculty of Petroleum Engineering, Petroleum University of Technology (PUT), Ahwaz, Iran
- Department of Petroleum Engineering, Faculty of Engineering, Soran University, Soran, Kurdistan Region, Iraq
- Department of Petroleum Engineering, College of Engineering, Knowledge University, Erbil, Kurdistan Region, Iraq
- School of Engineering, Edith Cowan University, Joondalup, WA 6027, Australia

#### 1 Introduction

Consumption of oil, the most common energy source, has been increased in the world and discovery of new oil reservoirs has been reduced due to exploration difficulties (Ali et al. 2018a). Thus, the oil industry focuses more on increasing the production from the currently producing reservoirs using different oil recovery methods including primary, secondary, and tertiary recovery processes (Ali et al. 2018b). In the primary phase, oil is usually recovered using the internal energy of the reservoir, while, water and gas injections are secondary methods used to maintain the reservoir pressure and increase the recovery factor after the decline of the reservoir. As is obvious, the primary and secondary recovery techniques enable the production of only about one-third of the oil from the reservoir (Kamal et al. 2017; Emadi et al. 2018; Ali et al. 2019a). Hence, EOR processes, such as thermal recovery, chemical recovery, miscible and immiscible flooding play a great role in extracting some of the remaining crude oil and improving oil recovery. Chemical



EOR techniques (cEOR) have been attracted more attention nowadays due to having different challenges including IFT reduction, wettability alteration, and adsorption behavior (Ali et al. 2019b; Nowrouzi et al. 2018, 2019). Selecting an appropriate EOR technique to be effective in reality can be done using screening criteria and screening algorithms (Mashayekhizadeh et al. 2014). Among all cEOR methods, surfactant flooding is the most effective chemical EOR method having the greatest potential to improve oil recovery. During surfactant flooding, the force that lowers the interfacial tension (IFT) and alters the wettability tends to allow the trapped crude oil in the pore spaces to be displaced (Howe et al. 2015; Manshad et al. 2016; Ahmadi and Shadizadeh, 2018; Hanamertani et al. 2017; Olayiwola and Dejam 2019a, b; Najimi et al. 2019).

In chemical EOR, many chemicals including surfactants, polymers, and alkalis are used to modify the displacement efficiency and the volumetric sweep efficiency. The displacement (microscopic) efficiency consists of the ability of the displacing fluid to sweep out crude oil in the reservoir, horizontally and vertically, toward the production wells (Kamal et al. 2015). This can be achieved by controlling the mobility ratio between oil and injected fluid (Dejam 2018, 2019). For this purpose, polymers as highly viscous solutions are usually injected into oil reservoirs (Saboorian-Jooybari et al. 2015). Meanwhile,

the displacement of oil at the pore scale is related to the volumetric sweep (microscopic) efficiency of the recovery process, which is controlled by the capillary forces and viscous forces. The capillary numbers are developed from a relationship between these two forces dependent on the viscosity, interfacial tension (IFT), and contact angle (Wang et al. 2010; Bera et al. 2013). According to Kamal et al. (2017), increasing the capillary numbers from  $10^{-7}$  and  $10^{-6}$  to about  $10^{-3}$  and  $10^{-2}$  will reduce the oil saturation by 90% and to zero. To reach these ranges, IFT between oil and water must be reduced to about 20-30 mN/m, which can be achieved by injecting the surfactant. Surfactant flooding also has an impact on micro-emulsification, wettability alteration, and mobility ratio (Kumar and Mandal 2018; Ahmadi and Shadizadeh 2013; Ahmadi et al. 2015). Numerous types of surfactants (cationic, anionic, and non-ionic) have been investigated in the laboratory and at the field scale based on the surfactant structure, adsorption and cost, reservoir temperature, salinity and pH, rock properties and the oil recovery (Table 1). In this study, two newly synthesized ecofriendly surfactants were used to improve the oil recovery by their IFT reduction and wettability alteration. Rostami et al. (2017) studied the effect of lysine derivative aminoacid surfactant on IFT reduction and wettability alteration; wherein IFT reduced from 35 to 19.6 mN/m, and

Table 1 Summary of previous works on effects of various surfactants on interfacial tension (IFT), contact angle, and oil recovery

Surfactant	IFT, mN/m Contact angle, degree		e, degree	Oil recovery, %	References	
	Without surfactant	With surfactant	Without surfactant	With surfactant	OOIP	
[C12mim][C1]	15.59	0.07	_		62.1	Nabipour et al. (2017)
[C18mim][Cl]	15.59	0.15	_		_	
AN-120	15.59	0.12	_		_	
NX-610	15.59	1.20	_		_	
NX-1510	15.59	0.36	_		_	
NX-2760	15.59	0.13	_		_	
TR-880	15.59	0.11	_		_	
CTAB	21.00	0.01	76.3	8	_	Kumar and Mandal (2016)
SDS	21.00	0.03	76.3	4	_	
TWEEN 80	21.00	0.14	76.3	10	_	
[C12mim][Br]	43.97	9.10	_		_	Nandwani et al. (2017)
[C14mim][Br]	43.97	7.20	_		_	
[C16mim][Br]	43.97	4.70	_		75.6	
CTAB	43.97	7.70	_		71	
Lysine derivative	35.00	19.58	160	119	53.19	Rostami et al. (2017)
L-Arginine	32.47	17.76	126.3	103.7	_	Takassi et al. (2017)
Cedar	30.1	7.1	_		15	Daghlian et al. (2016)
CTAB	30.1	Ultralow	_		17	
SDS	30.1	7.2	_		_	
AOS	30.1	6.0	_		13	



the wettability of the rock changed toward water-wet by decreasing the contact angle from 160° to 119°, and consequently, the oil recovery was increased to 53.9% OOIP. Nabipour et al. (2017) used two anionics ([C12mim][C1] and [C18mim][C1]) and five most common (AN-120, NX-610, NX-1510, NX-2760, and TR-880) surfactants to reduce IFT and increase oil recovery. Their results showed that the minimum IFT was 0.07 mN/m and a maximum oil recovery up to 62.1% OOIP were achieved using an anionic surfactant with a concentration of 4000 ppm (Nabipour et al. 2017). Additionally, Daghlian et al. (2016) investigated the effect of a natural surfactant called Cedar and three common surfactants (CTAB, SDS, and AOS) on IFT reduction. IFT was reduced from 30.1 to about 6 mN/m and ultralow values with increasing oil recovery up to 17% OOIP. Kumar and Mandal (2018) synthesized a zwitterionic surfactant for improving oil recovery from carbonate reservoirs; they identified a significant reduction in IFT value and altered the wettability of rock from oil-wet to water-wet with additional oil recovery of 30.8% OOIP. More recently, Olayiwola and Dejam (2019a, b) stated that the role of chemical processes (i.e., surfactant) in improving oil recovery can be improved by adding nanoparticles.

The ultimate goal of this study is to investigate the effects of two synthetic eco-friendly surfactants called lauroyl arginine (L-Arg) and lauroyl cysteine (L-Cys) on improving oil recovery from carbonate reservoirs. The synthesized surfactants were examined using Fourier transform infrared spectroscopy (FT-IR) and nuclear magnetic resonance (NMR). The effects of L-Arg and L-Cys surfactants at different concentrations on IFT reduction, wettability alteration, and oil recovery improvement have been experimentally investigated.

# 2 Experimental

The experimental work of this study was divided into three parts, as illustrated schematically in Fig. 1. These were (i) synthesis and characterization of eco-friendly surfactants, (ii) the preparation and CMC identification of surfactant solutions, and (iii) the IFT, contact angle, and coreflooding tests.

#### 2.1 Materials

All the salts and chemical reagents including arginine, cysteine, lauroyl chloride, methanol, toluene, ethanol, sodium dodecyl sulfate, sodium hydroxide, and sodium chloride with a purity of about 99% were purchased from Merck Company. The chemical structures of arginine and cysteine are shown in Fig. 2.

For preparing surfactant and brine solutions, distilled water with a density of 0.998 g/cm<sup>3</sup> and pH of 7.02 was used. Brine was prepared by mixing NaCl to 10,0000 ppm concentration with distilled water. The density and viscosity of the synthetic seawater (SSW) were about 1.068 g/cm<sup>3</sup> and 1.42 cP, respectively. In addition, crude oil with a density of 0.875 g/cm<sup>3</sup> (30° API) and a viscosity of 11 cP was obtained from the Kupal oilfield and used in coreflooding tests. However, for IFT and contact angle measurements, kerosene with

(a) NH O (b) O 
$$HS$$
 OH  $HS$  OH  $NH_2$ 

Fig. 2 Molecular structures of a arginine, and b cysteine

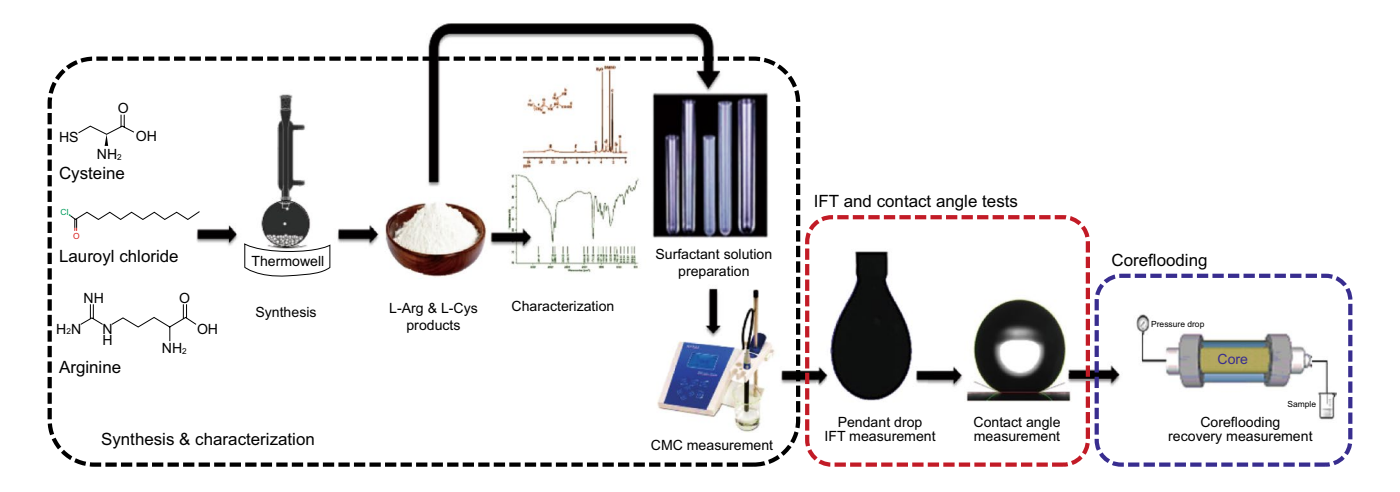


Fig. 1 Schematic illustration of experimental procedures of synthesizing L-Arg and L-Cys surfactants and their EOR applications



a density of 0.79 g/cm<sup>3</sup> and a viscosity of 1.32 cP was used instead of crude oil due to the lack of clarity in the surfactant color. For the wettability measurement and coreflooding, the core plugs and thin sections were collected from the Asmari Carbonate Formation outcrop from the Baba-kuhi Mountain in Iran.

# 2.2 Synthesis of amino-acid surfactants

Two amino-acid surfactants, lauroyl arginine (L-Arg) and lauroyl cysteine (L-Cys), were used as eco-friendly EOR agents in this study since they are non-toxic.

# 2.2.1 L-Arg synthesis

In order to synthesize L-Arg with accordance with Takassi et al. (2017) and Madani et al. (2019), 5 mL of lauroyl chloride and 3.0 mg of arginine were mixed with 100 mL of methanol in a 250-mL beaker. After mixing thoroughly for 2 h, the solution was transferred into a dry round-bottom flask and was mixed for 24 h by magnetic stirring at the reflux temperature when a white precipitate was observed in the bottom of the flask. Afterward, the white deposit was filtered and dried at 80 °C and atmospheric pressure. The collected powder of L-Arg was recrystallized from the distilled water—ethanol solvent.

#### 2.2.2 L-Cys synthesis

Using the method of Ramshini (2017), lauroyl cysteine (L-Cys) was synthesized by mixing 2 mg of cysteine and 100 mL of methanol in a round-bottom flask containing a magnetic stirring bar. First, the mixture was stirred for 1 h, but no dissolution of cysteine was observed. Then, 4 mL of lauroyl chloride was poured slowly into the flask and the cysteine completely dissolved in the methanol, and then the mixture was stirred for 12 h at room temperature. The produced L-Cys (a white colored precipitate) was separated by attaching a round-bottom flask to a vacuum pump on the magnetic stirrer rotated at 80 °C. Finally, the produced material was crystallized using the distilled water–ethanol mixture to obtain a purified powder.

#### 2.2.3 Characterization of amino-acid surfactants

After the purification of the produced material by crystallization in a distilled water–ethanol mixture, sufficient crystallized powder was extracted for melting point, nuclear magnetic resonance (<sup>1</sup>H-NMR) and Fourier transform infrared (FT-IR) spectra analyses (Takassi et al. 2017; Ramshini 2017; Madani et al. 2019). The melting point of the purified synthesized L-Arg surfactant was measured at 185–186 °C, which is a good indicator for the synthesis process, since the

formation of the target surfactant has effectively decreased the melting point of arginine. The product in that state was dispatched for FT-IR and <sup>1</sup>H-NMR spectra analysis tests. A Bomem MB-Series 1998 spectrophotometer (Quebec, Canada) was used to obtain the FT-IR spectrum of the sample applying the potassium bromide (KBr) pellet approach with a 4 cm<sup>-1</sup> resolution. A Bruker (Rheinstetten, Germany) Avance 500 spectrometer was used to record <sup>1</sup>H-NMR spectrum of the surfactant sample at ambient temperature in deuterated dimethyl sulfoxide (DMSO-d6) as solvent. Units of parts per million (ppm) denoted by  $\delta$  were utilized to show the chemical shifts in this spectrum. The number of protons (N) was reported for a specific resonance by NH. Multiplicities were also indicated as singlet (s), triplet (t), and multiplet (m). The melting point of the sample was determined in capillary tubes with a melting point device (Barnstead Electrothermal 9200, Dubuque, Iowa, USA). The melting point of L-Cys was 176–178 °C.

# 2.3 Preparation and CMC measurement of surfactant solutions

To prepare surfactant solutions, L-Arg and L-Cys were separately mixed with distilled water in a beaker using a magnetic stirrer (MR3001 K) for 30–60 min. The concentration of the surfactant solutions ranged from 200 to 10,000 ppm. Then, the densities of all the prepared surfactant solutions were measured using a DA-640 KEN density meter at ambient conditions (Table 2). In addition, the CMC values of both surfactants were determined by measuring the electrical conductivity, pH, and turbidity characteristics of surfactant solutions over a wide concentration range with a JEN-WAY-4510 conductivity meter, a Mettler Toledo pH-meter, and a AL250T-IR turbidity meter, respectively.

#### 2.4 IFT measurement

The pendant drop method is a suitable simple method that can be used to measure IFT between liquid and liquid or liquid and gas. The pendant drop method can measure both static and dynamic IFT. This method measures the IFT using an analysis of the drop shape (Bagalkot et al. 2018):

$$\sigma = \frac{\Delta \rho g D^2}{H} \tag{1}$$

where  $\Delta \rho$  is the difference in density between the two fluids, g is the acceleration of gravity, D is the maximum diameter of the droplet, and H is the drop shape coefficient.

A VIT-6000 device manufactured by Fars Company with a high accuracy of 99% was used to measure the value of IFT between liquid–liquid systems in both static and dynamic conditions (Fig. 3). In this study, the IFTs between



Table 2	Formulation	of I-Arg and	L-Cvs surfactant	colutione use	d in this study
iablez	FOITHUIAHOII	OLL-AIR AIR	L-C vs surfactant	. SOIULIOHS USE	a in this study

L-Arg sample	Surfactant concentration, ppm	Density, g/cm <sup>3</sup>	L-Cys sample	Surfactant concentration, ppm	Density, g/cm <sup>3</sup>
L-Arg-200	200	0.9986	L-Cys-200	200	0.9985
L-Arg-400	400	0.9987	L-Cys-400	400	0.9986
L-Arg-600	600	0.9988	L-Cys-600	600	0.9987
L-Arg-800	800	0.9989	L-Cys-800	800	0.9988
L-Arg-1000	1000	0.9991	L-Cys-1000	1000	0.9989
L-Arg-2000	2000	0.9994	L-Cys-2000	2000	0.9993
L-Arg-4000	4000	0.9998	L-Cys-4000	4000	0.9998
L-Arg-6000	6000	1.0001	L-Cys-6000	6000	1.0002
L-Arg-8000	8000	1.0008	L-Cys-8000	8000	1.0011
L-Arg-10000	10,000	1.0012	L-Cys-10000	10,000	1.0017



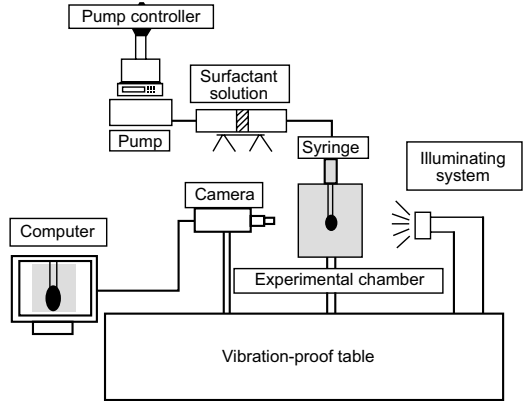


Fig. 3 A schematic diagram of a VIT-6000 apparatus used to measure IFT and contact angle

kerosene and surfactant solutions with different concentrations (200–10,000 ppm) were measured. IFT measurements were simply performed as follows: (1) kerosene and surfactant solutions with different concentrations were prepared; (2) they were stored in the solution injection chambers; (3) first, kerosene was pumped into the main chamber of the device; (4) the surfactant solution was then injected from the injection chamber into the needle device in order to provide a drop of the surfactant solution on the end of the needle to be hung inside the kerosene phase; and (5) the IFT measurement between kerosene and the surfactant solution was performed.

#### 2.5 Contact angle measurement

The contact angle is one of the quantitative methods which identifies the wetting of the reservoir rock in the presence of two fluids. This method is the most common wettability measurement in the oil industry. It can be performed under different pressure and temperature conditions (Tiab and Donaldson 2016). In the current work, a VIT-6000 apparatus was used to

measure the contact angle at a temperature of 70–80 °C and a pressure of 1200 psi (Fig. 3). For this purpose, a carbonate rock thin section with a diameter of 2 mm were trimmed from the carbonate outcrop sample and polished to become entirely smooth. The prepared rock sections were then cleaned with toluene and distilled water to remove all impurities, and as outlined by Villard et al. (1993) and Manshad et al. (2017), they were aged in kerosene at 70 °C for 12 days to become oilwet. In order to change the wettability of oil-wetted rock slices under static conditions, they were submerged in enclosed containers filled with surfactant solutions (L-Arg and L-Cys) for 5 days. The wettability of carbonate rock sections was qualitatively assessed by measuring the contact angle of a kerosene droplet on the surface of the prepared rock thin sections, before and after the treatment with surfactant solutions.

#### 2.6 Coreflooding test

Figure 4 illustrates a schematic diagram of the coreflooding setup. The device is mainly composed of tanks containing



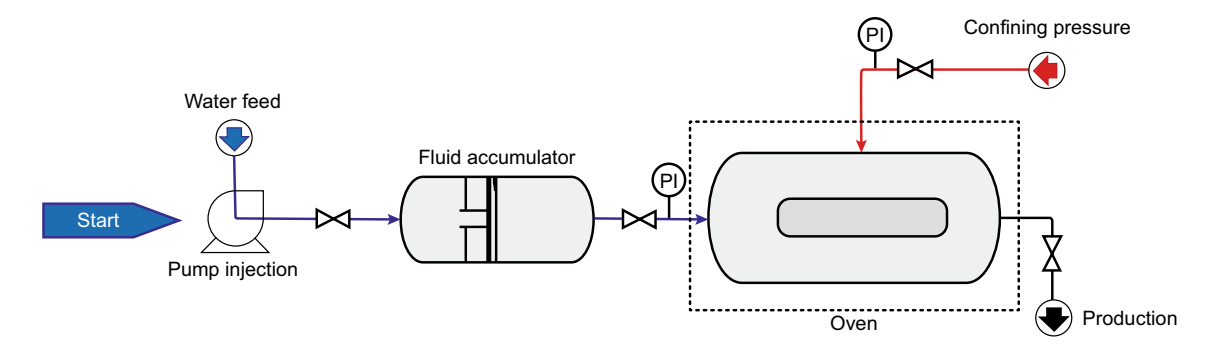


Fig. 4 A schematic diagram of the coreflooding apparatus

injection fluids, pumps, a core holder, and a produced-oil collector. Fluids from their chambers are pumped into the core plug. In this research, the core chamber can hold a core plug with a maximum length of 3.5 in and a maximum diameter of 1.5 in. The coreflooding was performed at 75 °C and 1500 psi. Fluid accumulators containing crude oil, brine, and surfactant solutions are located along with a core holder inside an oven to control the temperature of the system. The output line of the core holder chamber is removed from the oven and the outlet fluid is stored in a special fluid collection vessel. In order to conduct displacement tests, carbonate core plugs with porosity of 9.3%–13.2% and permeability of 7.6–10.4 mD were selected from the Asmari outcrop in Iran. The selected plugs were cleaned with toluene using Soxhlet extraction at 80 °C for 24 h in order to remove the presence of water, oil, and any other residues. Then the core samples were dried in an oven at 120 °C for 24 h. Displacement tests were conducted on core plugs at 75 °C. The experimental procedures are as follows: (1) 1.6 pore volume (PV) of brine (100,000 ppm NaCl solution) was injected into the core plug at a flow rate of 0.5 cm<sup>3</sup>/min (as a secondary recovery). Two pressure transducers were used to record the pressure values at the injection and production points. (2) Afterward, 1.4 PV surfactant solution (as a tertiary recovery, L-Arg-2000 or L-Cys-4500 solution) was injected into the core plug at a flow rate of 0.3 cm<sup>3</sup>/min. The oil recovery factors (RF) of both brine injections and L-Arg-2000 and L-Cys-4500 surfactant flooding were determined from the volume of the oil collected from the outlet of the coreflooding apparatus.

# 3 Results and discussion

# 3.1 Spectral characterization of synthesized surfactants

The mechanisms of synthesizing L-Arg and L-Cys surfactants are shown in Fig. 5. FT-IR and 1 H-NMR spectroscopy were used to confirm the structure of the synthesized amino-acid-based-surfactant, as shown in Figs. 6 and 7. Figure 6a

shows the FT-IR spectrum of the produced L-Arg revealing the absorption peak of the amine group at 3341 cm<sup>-1</sup>. The absorption band at 2927 cm<sup>-1</sup> was a characteristic peak for aliphatic hydrogens. The carbonyl peak of the carboxylic acid group appeared at 1743 cm<sup>-1</sup> which was overlapped by that of amide carbonyl groups. The peaks at 1589 and 1511 cm<sup>-1</sup> were ascribed to N-H asymmetric and symmetric in-plane bending of amide and amine groups, respectively. The peak at 1445 cm<sup>-1</sup> could be attributed to vibration of the amino group which is in resonance with the attached amine group. The C-O stretching band was observed at 1057 cm<sup>-1</sup> and a peak appeared at 729 cm<sup>-1</sup> due to the N-H out of plane bending (Takassi et al. 2017; Madani et al. 2019). Additionally, Fig. 6b illustrates the FT-IR spectrum of L-Cys surfactant, absorption of the amine group appeared at around 3433 cm<sup>-1</sup>. The absorption band at 2955 cm<sup>-1</sup> was the characteristic peak for aliphatic hydrogens. The weak absorption peak at 2379 cm<sup>-1</sup> was due to the S-H stretching vibration. The carbonyl peak of the amide group and carboxylic acid group appeared at 1637 and 1715 cm<sup>-1</sup>. The peaks at 1541 and 1509 cm<sup>-1</sup> were ascribed to N-H asymmetric and symmetric in-plane bending of amide groups, respectively. The C-O stretching band could be observed at 1280 cm<sup>-1</sup> and the peak that appeared at 792 cm<sup>-1</sup> was due to the N-H out of plane bending (Ramshini 2017).

Figure 7a presents the H-NMR spectrum of L-Arg, wherein the carboxyl proton was observed at 12.38 ppm. The NH protons of amide, imine, and amine groups were observed at 8.19, 7.39, and 7.17 ppm, respectively. The peak at 4.99 ppm is related to the chiral center proton. The methylene group attached to the amine group was observed at 3.00 ppm. The peak at 2.87 ppm was due to the methylene group attached to the amide group. Some of the peaks of the methylene protons and one of the amine groups were merged together. The resonance of these protons was observed at around 1.81–1.39 ppm. The methyl group of the hydrocarbon tail was also observed as a triplet peak at 0.90 ppm (Takassi et al. 2017; Madani et al. 2019). In the H-NMR spectrum of the developed L-Cys, the carboxyl proton was



Fig. 5 Mechanisms of synthesized surfactants. a L-Arg. b L-Cys

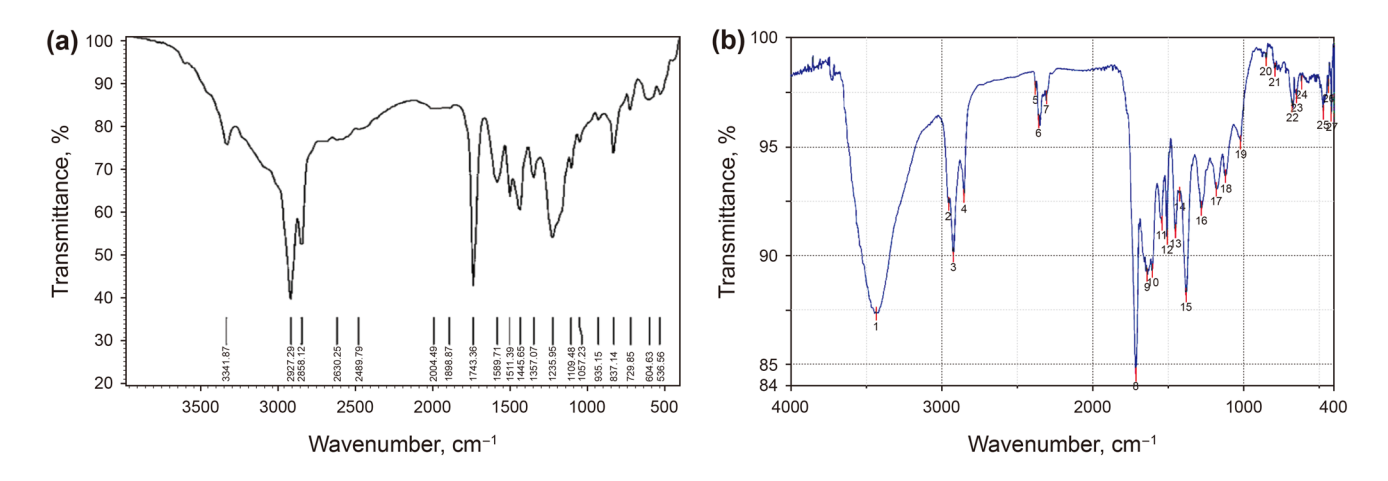


Fig. 6 FT-IR spectrum of the synthesized amino-acid surfactants. a L-Arg (Takassi et al. 2017; Madani et al. 2019). b L-Cys (Ramshini 2017)

observed at 12.48 ppm. The appearance of the NH proton of amide group at 8.335 ppm as a peak indicated the presence of an amide group in the surfactant structure. The proton of the chiral center appeared as a doublet of the doublet in the range of 4.79–4.81 ppm. The resonance of the diastereotopic hydrogens bonded to the neighboring carbon of the chiral

center appeared in the range of 3.12–3.31 ppm. The peaks of the methylene protons of the dodecanoyl chain were merged together. The resonance of these protons was observed at around 2.01–2.28 ppm. The SH proton was observed at 1.50 ppm and also the methyl group of the hydrocarbon tail was observed at 0.88 ppm (Ramshini 2017).



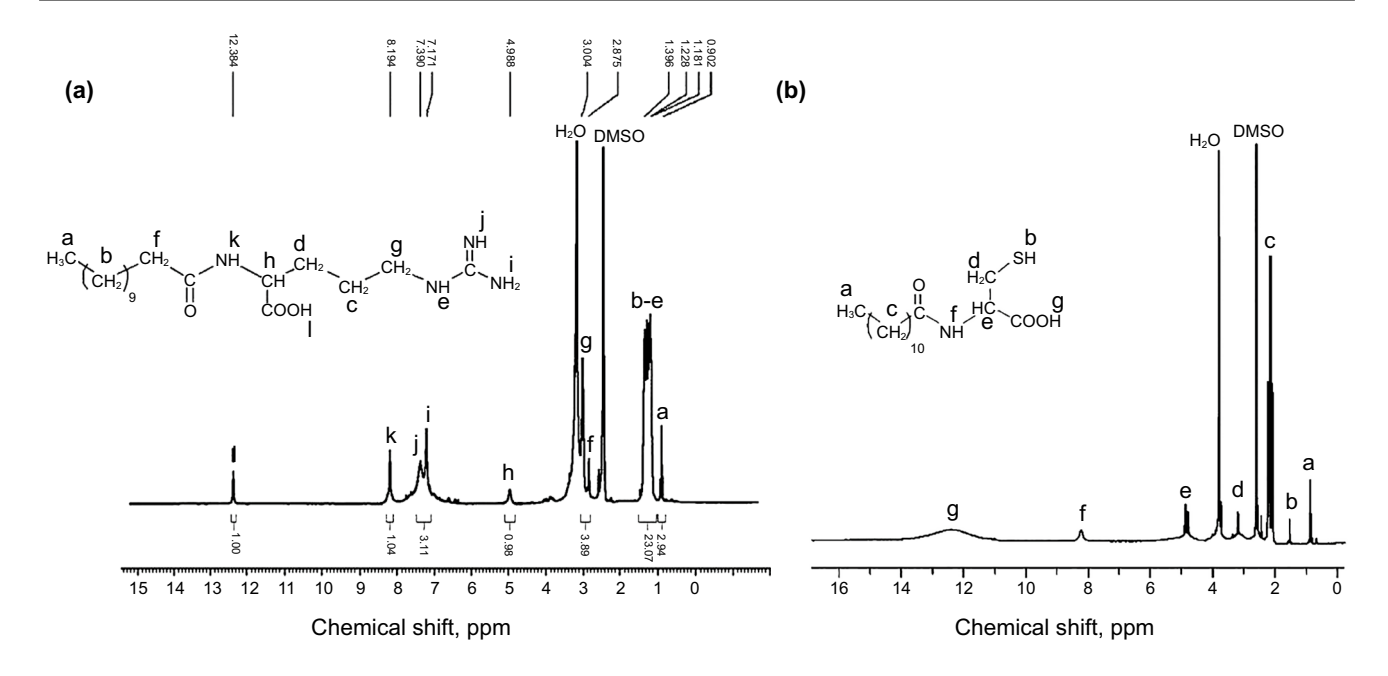


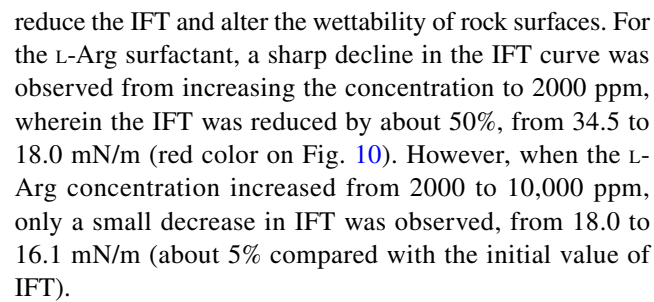
Fig. 7 H-NMR spectrum of the synthesized amino-acid surfactants. a L-Arg (Takassi et al. 2017; Madani et al. 2019). b L-Cys (Ramshini 2017)

#### 3.2 Characterization of surfactant solutions

In this part, the characteristics of the prepared surfactant solutions (200–10,000 ppm) including conductivity, pH, and turbidity were measured to identify the critical micelle concentrations (CMC). Figure 8 illustrates the results of conductivity, pH, and turbidity of the L-Arg solutions. As it can be seen, the optimum values of the CMC from conductivity, pH, and turbidity were 1700, 1900, and 2200 ppm, respectively. Although there is a small difference among the values of CMC dependent on the three measured properties of solutions, 2000 ppm was selected as an average effective value of the CMC for the solution prepared from L-Arg. The measured properties of the L-Cys solutions at different concentrations of 200, 400, 600, 800, 1000, 2000, 4000, 8000, and 10,000 ppm were shown in Fig. 9. From the conductivity, pH, and turbidity curves, different values of CMC were determined which were 5200, 4400, and 4500 ppm, respectively. Accordingly, the concentration of 4500 ppm has been chosen as the effective CMC for the L-Cys solution.

#### 3.3 IFT

Figure 10 shows IFT curves of L-Arg and L-Cys solutions. Surfactant solutions were prepared using different concentrations of the synthesized amino-acid surfactants. The selected concentrations were 200, 400, 600, 800, 1000, 2000, 4000, 8000, and 10,000 ppm. The value of IFT decreased with an increase in the surfactant concentration, which is similar to the results discussed by Pal et al. (2018) where they used a synthesized sodium ethyl ester sulfonate surfactant to



The measured values of IFT between kerosene and L-Cys solutions (blue solid circles) are also shown in Fig. 10. Although the CMC of L-Cys is higher compared with the L-Arg (Figs. 8, 9), its IFT curve shows a similar trend to the L-Arg IFT curve as shown in Fig. 10. Additionally, a sharp reduction in the IFT value was observed from the zero to 4000 ppm of L-Cys. From the initial value 34.5 mN/m, the IFT was decreased to 15.4 mN/m at the CMC concentration. Totally, both types of the surfactants demonstrated the same performance in reducing IFT. Shapes of kerosene droplets within both L-Arg and L-Cys solutions are illustrated in Fig. 11.

## 3.4 Contact angle

The contact angle values between kerosene and the prepared surfactant solutions of different concentrations are shown in Fig. 12. The measured contact angles (Fig. 12a) between kerosene and L-Arg solutions reduced from 144° to 70°. It is also clear that a rapid drop in the value of contact angle occurred with increasing the L-Arg concentration up to 2000 ppm (from 144° to 78°), and this decline continued



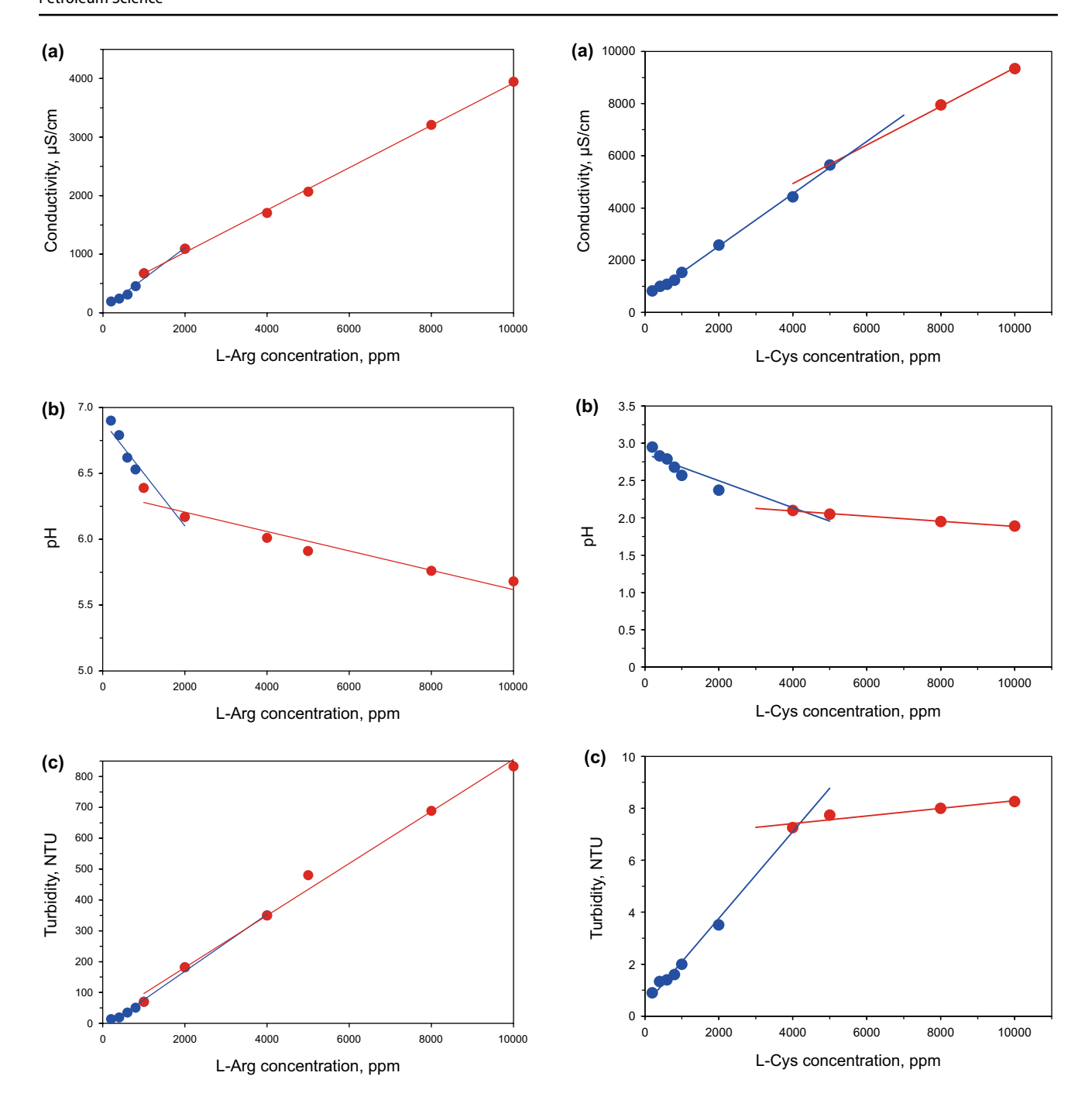


Fig. 8 CMC determination of the L-Arg solution via different methods. a Conductivity.  $b\ pH.\ c$  Turbidity

Fig. 9 CMC determination of the L-Cys solution. a Conductivity. b pH. c Turbidity

very smoothly to 70° at 10,000 ppm concentration. This is quite consistent with the descriptions of Mandal et al. (2015), wherein they used a mixed Tween 80 and SDBS solution to alter the wettability of quartz rocks. In addition, while using L-Cys solutions, the contact angle between kerosene and surfactant solutions decreased gradually and significantly from 144° to 75° at the CMC point (4000 ppm concentration), as shown in Fig. 12b. While, above the CMC

point, the value of the contact angle changed only slightly. Generally, both used surfactants were active in reducing the contact angle and changing the wettability toward water-wet.

# 3.5 Coreflooding

In this study, surfactant solutions were prepared by dispersing the synthesized surfactant in water at different



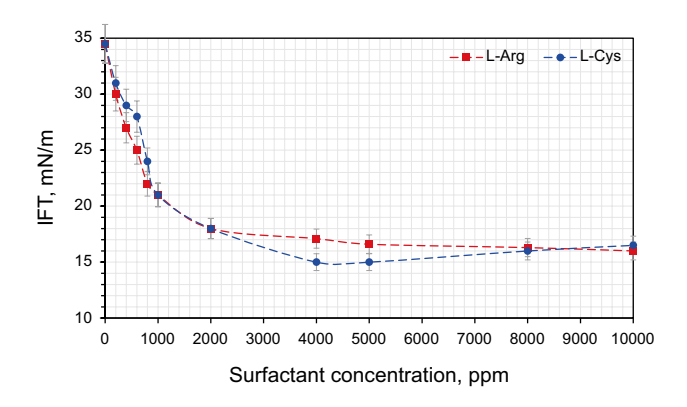


Fig. 10 IFT values measured between kerosene and L-Arg and L-Cys solutions at concentration of 200–10,000 ppm

concentrations (200–10000 ppm). The CMC for L-Arg and L-Cys surfactants were determined from the results of conductivity, pH, and turbidity. The minimum IFTs and contact angles of L-Arg and L-Cys were measured at their CMCs, 2000 and 4500 ppm, respectively. These L-Arg-2000 and L-Cys-4500 solution were selected to be injected after water injection (Table 3). For this purpose, two core plugs were prepared and their properties are listed in Table 3.

Flooding profiles in Fig. 13 illustrate that an oil recovery of 38.6% OOIP was achieved after injecting 1.6 PV of brine into Plug #1; and a follow-up injection of 1.4-PV L-Arg-2000 solution recovered an additional 11.9% OOIP for a total oil recovery 50.5% OOIP (green and black lines in Fig. 13). However, from Plug #2, 43.7% OOIP was recovered by water injection, and an additional 8.9% OOIP was produced by the tertiary flooding of L-Cys-4500, as shown by red and blue lines in Fig. 13. These improvements in oil recovery could be due to the IFT reduction and wettability alteration. Generally, L-Arg-2000 surfactant (11.9% OOIP) provided a better recovery performance than L-Cys-4500 surfactant (8.9% OOIP). This may be due to higher adsorption of the L-Cys-4500 than that of L-Arg-2000 onto the rock surface.

# 4 Conclusions

In this study, the effects of lauroyl arginine (L-Arg) and lauroyL cysteine (L-Cys) surfactants on the IFT reduction, wettability alteration and oil recovery were studied. The IFT and wettability were measured using the pendant drop method and the contact angle method, also oil recovery was determined by coreflooding tests. The outcomes of this study are summarized as follows:

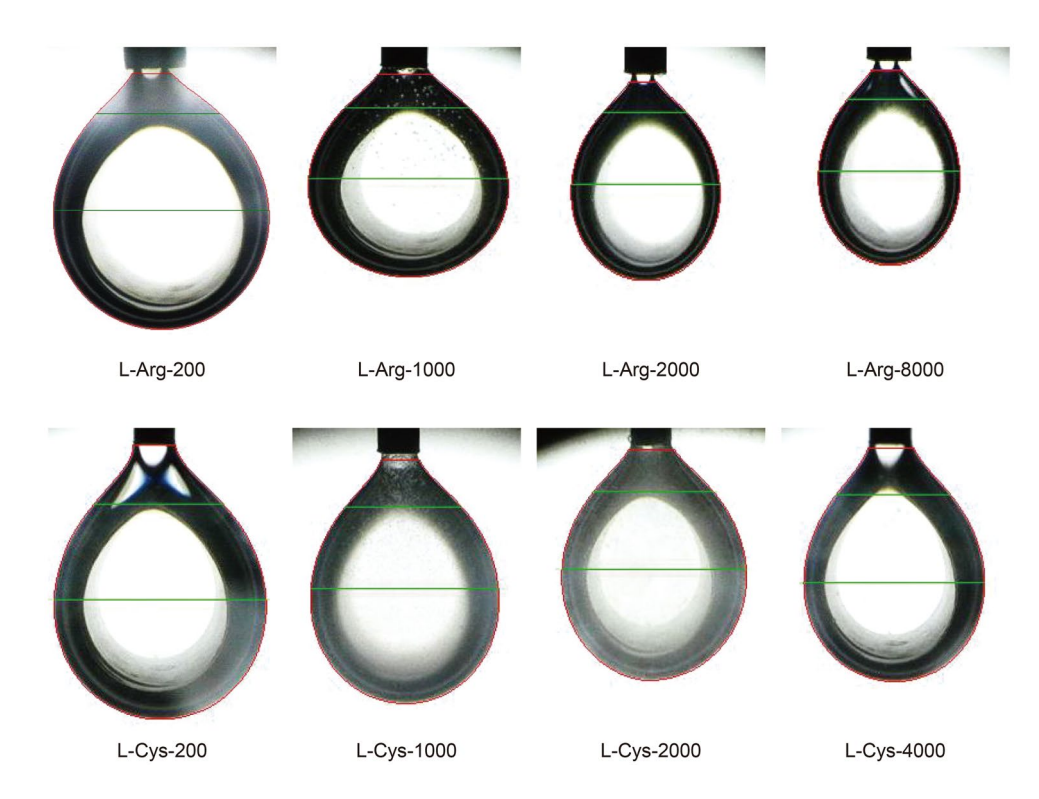


Fig. 11 Shape profiles of kerosene droplets against surfactant solutions



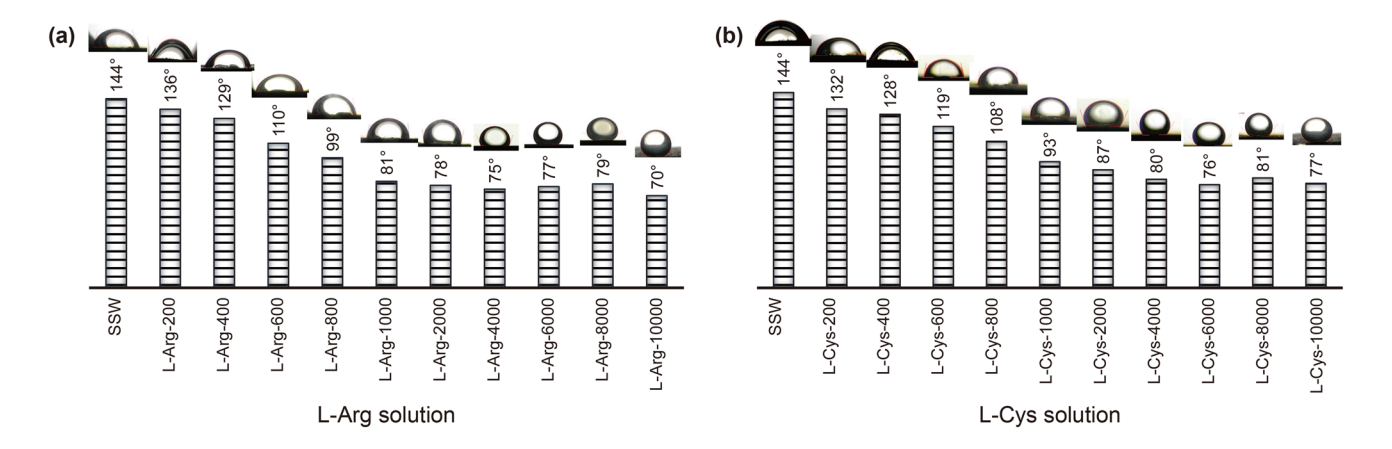


Fig. 12 Contact angle between kerosene and a L-Arg and b L-Cys solutions at different concentrations

Table 3 Summary of secondary and tertiary flooding

Core	Porosity, %	Permeability, mD	Pore volume (PV), cm <sup>3</sup>	S <sub>oi</sub> ,%	Injection fluid	Water floodin Oil recovery, % OOIP		Surfactant flo Oil recovery, % OOIP		Total oil recovery, %OOIP
Plug #1	13.097	10.41	12.74	72.2	L-Arg-2000	38.6	44.3	11.9	35.7	50.5
Plug #2	9.314	7.68	9.08	74.3	L-Cys-4500	43.7	41.9	8.9	35.2	52.6

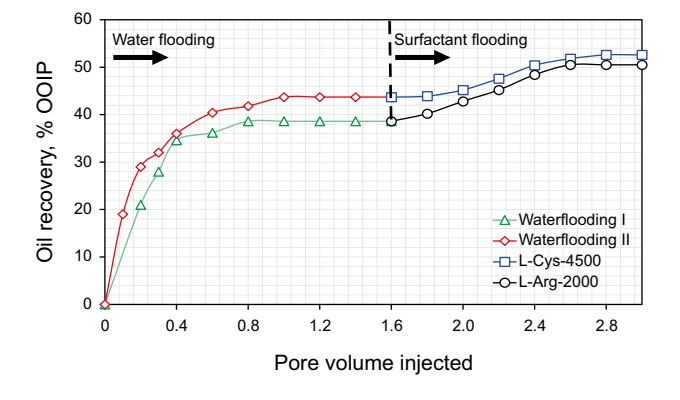


Fig. 13 Oil recovery profiles of water injection, L-Arg-2000 and L-Cys-4500 flooding into the Asmari core plugs. The green line represents the first brine injection into Plug #1, the red line shows the recovery from the second brine injection into Plug #2, the black line is for the L-Arg solution injection at 2000 ppm into Plug #1 after the first brine injection, and the blue line demonstrates the L-Cys solution injection at 4500 ppm into Plug #2 after the second water injection

- CMCs of L-Arg and L-Cys solutions were measured to be 2000 and 4500 ppm, respectively, from electrical conductivity, pH, and turbidity measurements.
- Both surfactants showed almost the same performance in reducing the value of IFT, which was about 55% from 35 to 15 mN/m. The highest efficiency of surfactant was achieved at different CMCs.

- The contact angle of the carbonate thin section was decreased slightly more by L-Arg than by the L-Cys surfactant at CMCs from 144° to 70° and 77°, respectively.
- L-Arg surfactant enabled the production of more additional crude oil compared to the L-Cys surfactant at their CMCs. L-Arg-2000 improved oil recovery from 38.6% to 50.5% OOIP (extra 11.9% OOIP), while it was increased from 43.7% to 52.6% OOIP (extra 8.9% OOIP) by L-Cys-4500.
- Despite obtaining promising results in this study through getting almost the same performance of L-Arg and L-Cys surfactants in reducing IFT and altering the wettability, L-Arg was more effective in improving oil recovery compared with L-Cys.

**Open Access** This article is distributed under the terms of the Creative Commons Attribution 4.0 International License (http://creativecommons.org/licenses/by/4.0/), which permits unrestricted use, distribution, and reproduction in any medium, provided you give appropriate credit to the original author(s) and the source, provide a link to the Creative Commons license, and indicate if changes were made.

# References

Ahmadi MA, Shadizadeh SR. Implementation of a high performance surfactant for enhanced oil recovery from carbonate reservoirs. J Pet Sci Eng. 2013;110:66–73. https://doi.org/10.1016/j.petro 1.2013.07.007.



- Ahmadi MA, Galedarzadeh M, Shadizadeh SR. Wettability alteration in carbonate rocks by implementing new derived natural surfactant: enhanced oil recovery applications. Transp Porous Media. 2015;106(3):645–67. https://doi.org/10.1007/s11242-014-0418-0.
- Ahmadi MA, Shadizadeh SR. Spotlight on the new natural surfactant flooding in carbonate rock samples in low salinity condition. Sci Rep. 2018;8(1):1–15. https://doi.org/10.1038/s41598-018-29321-w.
- Ali JA, Kolo K, Manshad AK, Mohammadi AH. Recent advances in application of nanotechnology in chemical enhanced oil recovery: effects of nanoparticles on wettability alteration, interfacial tension reduction, and flooding. Egypt J Pet. 2018a;27(4):1371–83. https://doi.org/10.1016/j.ejpe.2018.09.006.
- Ali JA, Kolo K, Manshad AK, Stephen KD, Keshavarz A. Modification of LoSal water performance in reducing interfacial tension using green ZnO/SiO<sub>2</sub> nanocomposite coated by xanthan. Appl Nanosci. 2018b. https://doi.org/10.1007/s13204-018-0923-5.
- Ali JA, Kolo K, Manshad AK, Stephen KD. Low-salinity polymeric nanofluid-enhanced oil recovery using green polymer-coated ZnO/SiO<sub>2</sub> nanocomposites in the Upper Qamchuqa Formation in Kurdistan Region, Iraq. Energy Fuels. 2019a;33(2):927–37. https://doi.org/10.1021/acs.energyfuels.8b03847.
- Ali JA, Kamal K, Manshad AK, Stephen KD. Potential application of low-salinity polymeric-nanofluid in carbonate oil reservoirs: iFT reduction, wettability alteration, rheology and emulsification characteristics. J Mol Liq. 2019b;284:735–47. https://doi. org/10.1016/j.molliq.2019.04.053.
- Bagalkot N, Hamouda NN, Isdahl OM. Dynamic interfacial tension measurement method using axisymmetric drop shape analysis. MethodsX. 2018;5:676–83. https://doi.org/10.1016/j.mex.2018.06.012.
- Bera A, Kumar T, Ojha K, Mandal A. Adsorption of surfactants on sand surface in enhanced oil recovery: isotherms, kinetics and thermodynamic studies. Appl Surf Sci. 2013;284:87–99. https://doi.org/10.1016/j.apsusc.2013.07.029.
- Daghlian JS, Sharifi SM, Sarapardeh AH. Toward mechanistic understanding of natural surfactant flooding in enhanced oil recovery processes: the role of salinity, surfactant concentration and rock type. J Mol Liq. 2016;222:632–9. https://doi.org/10.1016/j.molli q.2016.07.086.
- Dejam M. Dispersion in non-Newtonian fluid flows in a conduit with porous walls. Chem Eng Sci. 2018;189:296–310. https://doi.org/10.1016/j.ces.2018.05.058.
- Dejam M. Advective-diffusive-reactive solute transport due to non-Newtonian fluid flows in a fracture surrounded by a tight porous medium. Int J Heat Mass Transf. 2019;2019(128):1307–21. https://doi.org/10.1016/j.ijheatmasstransfer.2018.09.061.
- Emadi S, Shadizadeh SR, Manshad AK, Rahimi AM, Mohammadi AH. Effect of nano silica particles on interfacial tension (IFT) and mobility control of natural surfactant (Cedr Extraction) solution in enhanced oil recovery process by nano-surfactant flooding. J Mol Liq. 2018;248:163–7. https://doi.org/10.1016/j.molliq.2017.10.031.
- Hanamertani AS, Pilus RM, Idris AK, Irawan S, Tan IM. Ionic liquids as a potential additive for reducing surfactant adsorption onto crushed Berea sandstone. J Pet Sci Eng. 2017;162:480–90. https://doi.org/10.1016/j.petrol.2017.09.077.
- Howe AM, Clarke A, Mitchell J, Staniland J, Hawkes L, Whalan C. Visualising surfactant enhanced oil recovery. Colloids Surf A. 2015;480:449-61. https://doi.org/10.1016/j.colsurfa.2014.08.032.
- Kamal MS, Sultan AS, Hussein IA. Screening of amphoteric and anionic surfactants for cEOR applications using a novel approach. Colloids Surf A. 2015;476:17–23. https://doi.org/10.1016/j.colsu rfa.2015.03.023.
- Kamal MS, Hussein IA, Sultan AS. Review on surfactant flooding: phase behavior, retention, IFT, and field applications. Energy

- Fuels. 2017;31(8):7701–20. https://doi.org/10.1021/acs.energ yfuels.7b00353.
- Kumar S, Mandal A. Studies on interfacial behavior and wettability change phenomena by ionic and nonionic surfactants in presence of alkalis and salt for enhanced oil recovery. Appl Surf Sci. 2016;372;42–51. https://doi.org/10.1016/j.apsusc.2016.03.024.
- Kumar A, Mandal A. Characterization of rock-fluid and fluid-fluid interactions in presence of a family of synthesized zwitterionic surfactants for application in enhanced oil recovery. J Pet Sci Technol. 2018;549:1–12. https://doi.org/10.1016/j.colsu rfa 2018 04 001.
- Madani M, Zargar G, Takassi MA, Daryasafar A, Wood DA, Zhang Z. Fundamental investigation of an environmentally-friendly surfactant agent for chemical enhanced oil recovery. Fuel. 2019;238:186–97. https://doi.org/10.1016/j.fuel.2018.10.105.
- Mandal A, Kar S, Kumar S. The synergistic effect of a mixed surfactant (Tween 80 and SDBS) on wettability alteration of the oil wet quartz surface. J Dispers Technol. 2015;37(9):1268–76. https://doi.org/10.1080/01932691.2015.1089780.
- Manshad AK, Rezaei M, Moradi S, Nowrouzi I, Mohammadi AH. Wettability alteration and interfacial tension (IFT) reduction in enhanced oil recovery (EOR) process by ionic liquid flooding. J Mol Liq. 2017;248:153–62. https://doi.org/10.1016/j.molli q.2017.10.009.
- Manshad AK, Olad M, Taghipour SA, Nowrouzi I, Mohammadi AH. Effects of water soluble ions on interfacial tension (IFT) between oil and brine in smart and carbonated smart water injection process in oil reservoirs. J Mol Liq. 2016;223:987–93. https://doi.org/10.1016/j.molliq.2016.08.089.
- Mashayekhizadeh V, Kord S, Dejam M. EOR potential within Iran. Spec Top Rev Porous Media Int J. 2014;5(4):325–54. https://doi.org/10.1615/specialtopicsrevporousmedia.v5.i4.50.
- Najimi S, Nowrouzi I, Manshad AK, Farsangi MH, Hezave AZ, Ali JA, et al. Investigating the effect of [C8Py][C1] and [C18Py][C1] ionic liquids on the water/oil interfacial tension by considering Taguchi method. J Pet Explor Prod Technol. 2019;1:1. https://doi.org/10.1007/s13202-019-0688-8.
- Nabipour M, Ayatollahi S, Keshavarz P. Application of different novel and newly designed commercial ionic liquids and surfactants for more oil recovery from an Iranian oil field. J Mol Liq. 2017;230:579–88. https://doi.org/10.1016/j.molliq.2017.01.062.
- Nandwani SK, Malek NI, Lad VN, Chakraborty M, Gupta S. Study on interfacial properties of Imidazolium ionic liquids as surfactant and their application in enhanced oil recovery. Colloids Surf A Physicochem Eng Asp. 2017;516:383–93. https://doi. org/10.1016/j.colsurfa.2016.12.037.
- Nowrouzi I, Manshad AK, Mohammadi AH. Effects of dissolved binary ionic compounds and different densities of brine on interfacial tension (IFT), wettability alteration, and contact angle in smart water and carbonated smart water injection processes in carbonate oil reservoirs. J Mol Liq. 2018;254:83–92. https://doi.org/10.1016/j.molliq.2017.12.144.
- Nowrouzi I, Manshad AK, Mohammadi AH. Effects of ions and dissolved carbon dioxide in brine on wettability alteration, contact angle and oil production in smart water and carbonated smart water injection processes in carbonate oil reservoirs. Fuel. 2019;235:1039–51. https://doi.org/10.1016/j.fuel.2018.08.067.
- Olayiwola SO, Dejam M. A comprehensive review on interaction of nanoparticles with low salinity water and surfactant for enhanced oil recovery in sandstone and carbonate reservoirs. Fuel. 2019a;241:1045–57. https://doi.org/10.1016/j.fuel.2018.12.122.
- Olayiwola SO, Dejam M. Mathematical modelling of surface tension of nanoparticles in electrolyte solutions. Chem Eng Sci. 2019b;197:345–56. https://doi.org/10.1016/j.ces.2018.11.047.
- Pal N, Saxena N, Laxmi KVD, Mandal A. Interfacial behaviour, wettability alteration and emulsification characteristics of a novel



- surfactant: implications for enhanced oil recovery. Chem Eng Sci. 2018;187:200–12. https://doi.org/10.1016/j.ces.2018.04.062.
- Ramshini AH. Synthesis and study of a novel lauroyl cysteine surfactant as water-oil demulsifier and modeling with fuzzy logic design (Unpublished doctoral dissertation). PUT, Abadan, Iran; 2017.
- Rostami A, Hashemi A, Takassi MA, Zadehnazari A. Experimental assessment of a lysine derivative surfactant for enhanced oil recovery in carbonate rocks: mechanistic and core displacement analysis. J Mol Liq. 2017;232:310–8. https://doi.org/10.1016/j. molliq.2017.01.042.
- Saboorian-Jooybari H, Dejam M, Chen Z. Half-century of heavy oil polymer flooding from laboratory core floods to pilot tests and field applications. In: 2015 SPE Canada Heavy Oil Technical Conference, Calgary, Alberta, Canada, 9–11, 2015. https://doi.org/10.2118/174402-MS.
- Takassi MA, Zargar G, Madani M, Zadehnazari A. The preparation of an amino acid-based surfactant and its potential application as an EOR agent. Pet Sci Technol. 2017;35(4):385–91. https://doi.org/10.1080/10916466.2016.1238933.
- Tiab DJ, Donaldson AC. Petrophysics book, 4th edn. Amsterdam: Elsevier; 2016:8(3). https://doi.org/10.1016/b978-0-12-80318 8-9.00001-2.
- Villard JM, Buckley JS, Morrow NS, Gauchet R. Wetting and water-flood oil recovery of a moderately viscous crude oil. SCA1993-23. Society of Core Analysts; 1993. https://doi.org/10.2118/20263-ms.
- Wang Y, Zhao F, Bai B. Optimized surfactant IFT and polymer viscosity for surfactant-polymer flooding in heterogeneous formations.
  In: SPE Improved Oil Recovery Symposium, 24–28 Apr 2010, Tulsa, OK, USA; 2010. https://doi.org/10.2118/127391-MS.

